

Changes in chemical composition of cortical bone associated with bone fragility in rat model with chronic kidney disease

Yoshiko Iwasaki^{a,*}, Junichiro James Kazama^b, Hideyuki Yamato^{c,d}, Masafumi Fukagawa^e

^a Department of Health Sciences, Oita University of Nursing and Health Sciences, Oita, 870-1201, Japan

^b Division of Blood Purification Therapy, Niigata University Medical and Dental Hospital, Niigata, Japan, 951-8520, Japan

^c Biomedical Research Laboratories, Kureha Co., Ltd., Tokyo, 169-8503, Japan

^d Kureha Special Laboratory Co., Ltd., Fukushima, 974-8232, Japan

^e Division of Nephrology and Metabolism, Tokai University School of Medicine, Kanagawa, 259-1193, Japan

ARTICLE INFO

Article history:

Received 18 September 2010

Revised 10 February 2011

Accepted 4 March 2011

Available online 11 March 2011

Edited by: Toshio Matsumoto

Keywords:

Chemical composition

Bone mechanical property

Chronic kidney disease

ABSTRACT

Bone fragility is a complication of chronic kidney disease (CKD). Patients on dialysis have higher risk of fracture than the general population, but the reason remains obscure. Bone strength is determined by bone mass and bone quality. Although factors affecting bone quality include microarchitecture, remodeling activity, mineral content, and collagen composition, it remains unclear which factor is critically important for bone strength in CKD. We conducted an *in vivo* study to elucidate the factors that reduce bone mechanical property in CKD. Rats underwent thyroparathyroidectomy and progressive partial nephrectomy (TPTx–Nx). Bone mechanical property, bone mineral density (BMD), and cortical bone chemical composition (all in femur) as well as histomorphometry (in tibia) were determined. The storage modulus, which is a mechanical factor, was reduced in CKD model rats compared with controls that underwent thyroparathyroidectomy alone (TPTx). There were no differences in BMD and histomorphometric parameters between groups. However, cortical bone chemical composition differed: mineral to matrix ratio and carbonate substitution increased whereas crystallinity decreased in TPTx–Nx. In addition, enzymatic crosslinks ratio and pentosidine to matrix ratio also increased. These changes were significant in TPTx–Nx rats with most impaired renal function. Stepwise multiple regression analysis identified mature to immature crosslink ratio and crystallinity as independent contributors to storage modulus. Deteriorated bone mechanical properties in CKD may be caused by changes in chemical composition of the cortical bone, and is independent of BMD or cancellous bone microarchitecture.

© 2011 Elsevier Inc. All rights reserved.

Introduction

Bone fragility is a complication of chronic kidney disease (CKD). Patients on dialysis have approximately an overall four-fold higher risk of hip fracture than sex- and gender-matched individuals in the general population [1,2]. However, the reason remains obscure. Recently, there is increasing recognition that patients with predialysis CKD also experience an increased fracture burden [3–7]. In particular, Nickolas et al. [3] reported that participants in the Third National Health and Nutrition Examination Survey (NHANES III) who were aged over 50 and had an estimated GFR (eGFR) between 15 and 59 ml/min (stages 3 and 4 CKD) had two-fold higher risk for hip fracture than individuals without CKD. In addition, the 1-year mortality rate of hip fracture event was nearly two and a half times greater in dialysis patients compared with the general population [2]. Mittalhenkle et al. [8] reported that the mortality of dialysis patients who experienced a hip fracture was higher than non-fracture controls matched by age, history of cardiovascular

disease, and dialysis duration. Furthermore a recent report indicated that amongst older non-dialyzed persons, an eGFR less than 45 ml/min is associated with an almost 2-fold increase in hip fracture-related mortality [9]. Therefore elucidation of the pathogenesis of decreased bone strength in patients with CKD is important to improve survival of this patient population.

The strength of bone is determined by bone mass and bone quality. Bone mass is represented by bone mineral density (BMD) measured by dual-energy X-ray absorptiometry (DXA). Jassal et al. [10] reported that BMD was associated with renal function indicated by creatinine clearance (CCr), and this association was strongest at higher CKD stage. Nevertheless, the association between BMD level and bone fracture risk is generally not clearly defined in CKD patients [11]. Moreover, the progression of kidney dysfunction induces excess secretion of parathyroid hormone (PTH). Elevated PTH levels induce cortical bone catabolism and deterioration of cortical architecture that could reduce cortical BMD and increase cortical porosity [12]. In fact parathyroidectomy was associated with a significant lower risk for hip and other fractures in chronic hemodialysis patients [13]. These findings suggest that elevated PTH in kidney dysfunction may contribute to increasing fracture risk. On the other hand, a recent study from Japan

* Corresponding author at: Department of Health Sciences, Oita University of Nursing and Health Sciences, Megusuno 2944-9, Oita, 870-1201, Japan. Fax: +81 97 586 4385. E-mail address: iwasaki@oita-nhs.ac.jp (Y. Iwasaki).

[14] reported that the incidence of hip fracture in dialysis patients was independent of Ca or PTH levels. Thus, although parathyroid function may be one significant factor that affects bone strength, it may not be a critically important factor and that other yet unknown factors would also affect bone strength in CKD patients.

Bone quality is the characteristic of bone, and encompasses geometry and bone mass distribution, trabecular bone microarchitecture, accumulation of microdamage, bone remodeling activity or turnover, the amount of mineral, the orientation, and crosslink of collagen component [15]. The mineral and collagen compositions (material properties) contribute to the quality of bone tissue and the resulting biomechanical properties of bone [16,17]. Yerramshetty et al. [18] demonstrated the relationship between bone mineral crystallinity and mechanical properties. McCreadie et al. [19] also reported that bone tissue compositional differences in women are associated with osteoporotic fracture. However, whether changes in material properties occur in CKD and affect bone strength or fracture risk in CKD have not been reported. To elucidate these questions, we conducted an in vivo experimental study.

Materials and methods

Animal experimental design

A rat model of chronic kidney injury without hyperparathyroidism was produced using the methods described elsewhere [20]. Briefly, 13 week-old male Sprague–Dawley rats weighing approximately 350 g underwent thyroparathyroidectomy (TPTx) and two-stage 1/2, 3/4 or 5/6 subtotal nephrectomy (Nx) (n = 6 per group). As control, a group that underwent TPTx alone was also included. All TPTx and TPTx–Nx rats were given continuous infusion of a physiological level of 1–34 PTH (0.1 µg/kg/h, Peninsula laboratories, Talyo Way, San Carlos, CA) using a subcutaneously implanted Alzet osmotic mini pump (Model 2002; Alza Corp., Palo Alto, CA; pumps exchanged every two weeks), and subcutaneous L-thyroxin (Sigma Chemical Company, St. Louis, MO) 4 µg/kg body weight 3 times per week, beginning on the second day after TPTx. Administration was continued until completion of the study. From completion of the second nephrectomy to the end of study, the animal feed was CE-2 diet supplemented with 2% calcium (Ca) and 1% phosphorus (P) (TD-92095, Harlan Teklad, Madison, WI). The amount of food consumption was equalized among groups by pair-feeding; the amount of food given to TPTx rats was adjusted everyday to the amount consumed by TPTx–Nx rats on the previous day. At week 6 after the second Nx, all rats were sacrificed and blood and bone samples were collected. Femur and tibia were collected from each rat. The right femur was used for the following analyses: BMD, mechanical property, and chemical composition. Fig. 1 shows the point or region of each measurement. Tibia was used for bone histomorphometry. Urine was collected before sacrifice to measure creatinine clearance.

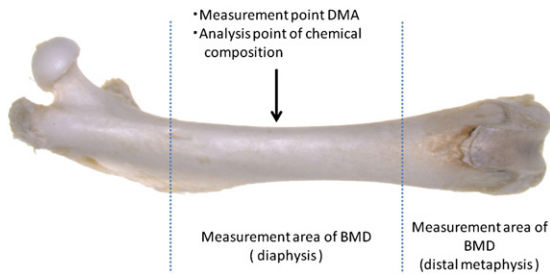
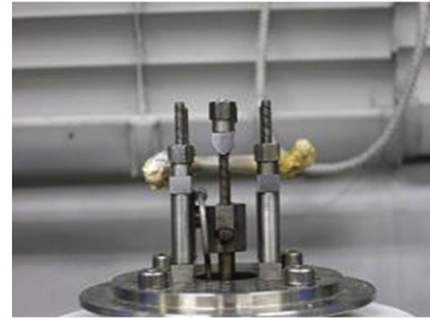


Fig. 1. Analyses performed on the femur and the region or point of each measurement. Right femur from each rat was used for BMD, mechanical property measurement, and chemical composition analysis.

(a)



(b)

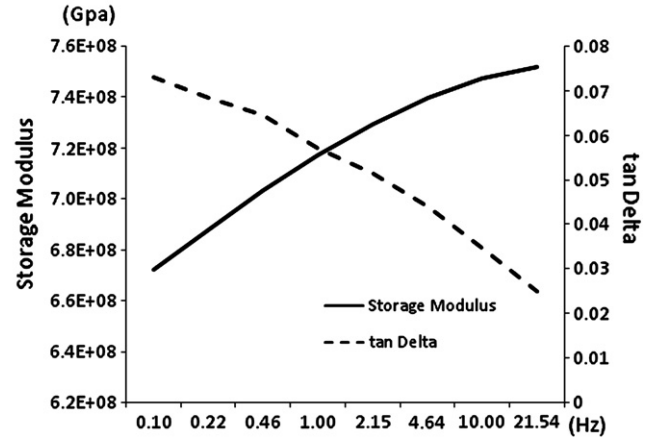


Fig. 2. DMA analysis: (a) sample placed on the DMA device; (b) standard profile of DMA. Both value of storage modulus and tan delta are dependent on the frequency of scanning.

Serum and urine biochemistry

Serum samples were stored at –70 °C until biochemical or hormonal assays. Urine samples were stored at –20 °C for later analyses. Serum calcium (Ca) and phosphorus (iP) were determined by the Calcium-E and Phospha-C assays (both from Wako Pure Chemicals, Tokyo Japan). Serum and urine creatinine concentrations were determined using Wako kit 277–1050, and urea nitrogen levels were measured using Wako kit 279–36201 (Wako Pure Chemicals). Serum PTH levels were measured with an immunoradiometric assay kit for rat PTH (Immutopics, San Clemente, CA). Serum levels of 1,25-dihydroxyvitamin D₃ [1,25(OH)₂D₃] were measured by a radioimmunoassay (RIA).



Fig. 3. Points of confocal Raman spectroscopic measurements on the femoral cross-sectional surface.

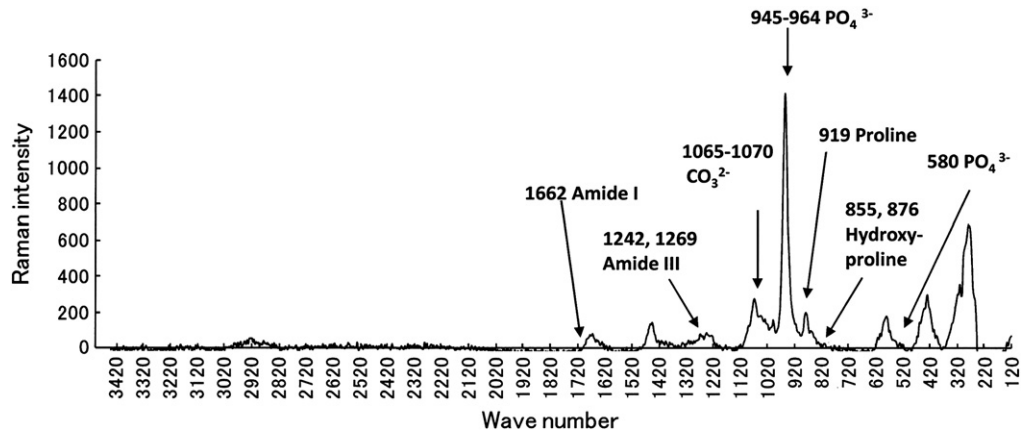


Fig. 4. Raman spectra of normal rat femur and band assignments.

Bone histomorphometry

Histomorphometric analysis of the secondary spongiosa was performed in the tibial proximal metaphysis between 1.2 and 3.6 mm distal to the growth plate-epiphyseal junction. A semiautomated system (Osteoplan II; Carl Zeiss, Thornwood, NY) was used, and measurements were made at $\times 200$ magnification. Parameters including cancellous bone volume (BV/TV, %), trabecular thickness (Tb.Th, μm), trabecular number (Tb.N, /mm), and trabecular separation (Tb.Sp, μm) were measured. Then, single-labeled surface (sLS/BS, %) and double-labeled surface (dLS/BS, %) were measured, and mineralized surface per total bone surface (MS/BS, %) was calculated. Labeling width was determined as the average distance between the double labels. Mineral apposition rate (MAR, $\mu\text{m}/\text{day}$) was calculated by dividing the labeling width by the number of days between the two calcein administrations. Bone formation rate per bone surface (BFR/BS, $\mu\text{m}^3/\mu\text{m}^2/\text{year}$) was the

product of $(\text{sLS}/2 + \text{dLS}) \times \text{MAR}/\text{BS}$. Trabecular osteoclast surface (Oc.S/BS, %) and eroded surface (ES/BS, %) were determined as parameters of bone resorption. The nomenclature, symbols, and units used in this study are those recommended by the American Society for Bone Mineral Research (ASBMR) Nomenclature Committee [21].

Measurement of BMD

Femoral bone samples were collected and all the connective tissues were carefully removed. BMD was measured by directly applying radiation beams. BMD of the right femur was determined by single energy X-ray absorptiometry using a bone mineral analyzer (DCS-600R; Aloka Co., Tokyo, Japan). BMD of the distal one-fourth of the femur, including the epi-metaphyseal region, and two- and three-fourths of the femur including the diaphysis region were measured.

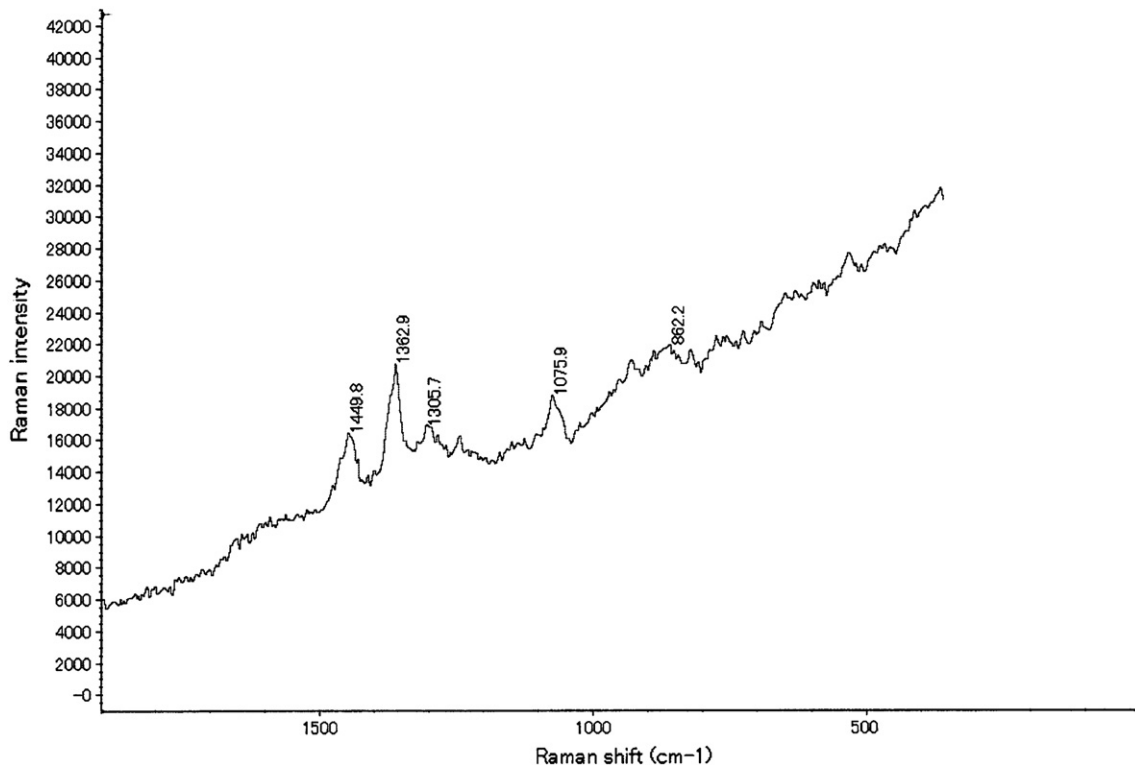


Fig. 5. Raman spectra of pentosidine standard and band assignments.

Measurement of storage modulus assessed by dynamic mechanical analysis (DMA)

Dynamic mechanical analysis (DMA) has been utilized to characterize cortical bone viscoelastic mechanical properties. This method is nondestructive and a specimen can be measured repeatedly at various frequencies using a dynamic mechanical analyzer while the specimen is subjected to very small nondestructive loads [22]. After BMD measurement, we determined viscoelastic mechanical properties of the femur. Before DMA, the thickness and width at the center of each femur were measured. Then the femur was placed in a dynamic mechanical analysis device (DMA 7e PerkinElmer, Norwalk, CT) and baseline viscoelasticity was measured in 0.9% saline solution at 37 °C by an oscillatory test using a 3-point bending configuration. Fig. 2 shows the femur sample placed in the DMA device and the standard profile of DMA analysis. Frequencies of scanning ranged from 1 to 10 Hz (in 0.2 Hz increments). The test was conducted under displacement control. Storage modulus E1, (obtained from dynamic test, equivalent to Young's modulus), loss factor, and tan delta (an indication of the amount of energy dissipated by viscous mechanisms relative to energy stored in the elastic component) were measured for each sample.

Confocal Raman spectroscopic measurements

Confocal laser Raman microspectroscopy [23] was used to examine the composition and relative amounts of the minerals and matrix produced in the femur. Raman spectroscopy is particularly useful for the analysis of mineral and matrix components in unprocessed bone preparations, in which these components are preserved [23]. A Nicolet Almega XR Dispersive Raman microscope system equipped with the OMNIC Atlas TM imaging software program (Thermo Fisher Scientific, MA, USA) was used, which permits mapping of an area smaller than 1 μm^3 on the bone microsurface of the cortical bone using the video microscopic stage control. High-brightness, low-intensity laser operating at 785 nm was used as the excitation source at a laser power of 35 mW. Each spectrum was the sum of ten 10-s measurements. The spectral resolution of the Almega XR under the above conditions was 3.58 cm^{-1} . After DMA measurement, each femur sample was cut at the center of the diaphysis. Raman spectroscopy was conducted on the cross-sectional surface. Fig. 3 shows the points of measurement on the femoral cross-sectional surface. For each sample, three averaged Raman spectral images were acquired in the middle of the anterior cortical bone (each image was acquired by ten 10-s measurements) and the average values were calculated.

Fig. 4 shows a typical Raman spectrum from a normal rat femur, and the prominent bands are labeled. The ν_1 phosphate stretching vibration at 950–964 cm^{-1} is the strongest marker for bone mineral. There was a strong band at 1065–1070, indicating type B carbonate substitution in the bone specimen (carbonate substituting for phosphate in the apatite lattice). The broad bands observed in the high-frequency region were amide III (1242 and 1269 cm^{-1}), the C–H bending mode (~1466 cm^{-1}), and amide I (1665 cm^{-1}). The amide I peak at 1665 cm^{-1} was mainly due to the presence of collagen. The phosphate symmetric stretch peak (at 950–964 cm^{-1}) was used to assess crystallinity of mineral, calculated as the inverse of the width of the phosphate band at half maximum intensity value using the same methods as previously reported [18,24]. Collagen maturity was estimated by the ratio of 1660 cm^{-1} to 1690 cm^{-1} [25], which indicates pyridinoline to dihydroxy-lysino-norleucine, both are enzymatic crosslinks of collagen. In addition, we recorded a spectrum of pentosidine standard (Fig. 5), which is a non-enzymatic crosslink of collagen. This pentosidine was purified and identified by high performance liquid chromatography (HPLC) and analyzed structurally by nuclear magnetic resonance (NMR) and fast atom bombardment (FAB) mass spectrometry [26]. We assigned major peaks and

Table 1
Creatinine clearance and serum biochemical parameters.

Parameters	TPTx (n=6)	TPTx-1/2Nx (n=6)	TPTx-3/4Nx (n=6)	TPTx-5/6Nx (n=6)
CCr (mL/min)	2.7 ± 0.2	1.6 ± 0.2*	1.3 ± 0.1*	1.0 ± 0.2*#
Cre (mg/dL)	0.6 ± 0.0	0.7 ± 0.1	1.0 ± 0.2*#	1.2 ± 0.2*#
BUN (mg/dL)	18.7 ± 2.1	26.3 ± 5.0	54.8 ± 10.8*#	71.0 ± 12.7*#
Ca (mg/dL)	10.4 ± 0.1	9.4 ± 2.2	9.8 ± 1.5	10.4 ± 1.1
iP (mg/dL)	8.2 ± 0.2	7.9 ± 1.7	8.8 ± 1.5	9.8 ± 2.3*
1,25(OH) ₂ D ₃ (pg/mL)	88.0 ± 10.1	81.0 ± 11.9	80.8 ± 11.1	78.8 ± 14.1
PTH (pg/mL)	108 ± 106	108 ± 58	103 ± 41	104 ± 64

TPTx; thyroparathyroidectomy, Nx; nephrectomy, TPTx-1/2Nx; thyroparathyroidectomized and 1/2 nephrectomized rats, TPTx-3/4Nx; thyroparathyroidectomized and 3/4 nephrectomized rats, TPTx-5/6Nx; thyroparathyroidectomized and 5/6 nephrectomized rats, CCr; creatinine clearance, Cre; creatinine, BUN; blood urea nitrogen, Ca; calcium, iP; inorganic phosphorus.

* p < 0.05 versus TPTx rats.

p < 0.05 versus TPTx-1/2Nx rats.

compared to previous report [27]. There were two major peaks at 1305 and 1362 in our pentosidine standard spectrum.

Statistical analysis

All data are expressed as mean ± SD, and a p value less than 0.05 was considered significant. Means of groups were compared by ANOVA, and significance of difference was determined by post hoc testing using Fisher's PLSD test. The association between mechanical property (storage modulus) and bone chemical composition parameters were investigated by simple linear regression followed by step-wise multiple regression analyses.

Result

Renal function and bone architecture

Significant increases in serum creatinine, urea nitrogen, and inorganic phosphate were observed in TPTx-5/6Nx rats compared with TPTx rats (Table 1). Creatinine clearance was significantly decreased in TPTx-3/4Nx and TPTx-5/6Nx rats compared with TPTx rats. In contrast, there were no significant differences in serum calcium, 1,25(OH)₂D₃ and PTH concentrations among four groups. There was no difference in the amount of food consumed among all groups (average intake: 23.8 g/day).

Cancellous bone histomorphometric features of the tibia are summarized in Table 2. No parameters showed significant differences among groups.

Table 2
Cancellous bone histomorphometric parameters.

Parameters	TPTx (n=6)	TPTx-1/2Nx (n=6)	TPTx-3/4Nx (n=6)	TPTx-5/6Nx (n=6)
BV/TV (%)	22.5 ± 2.2	24.8 ± 1.9	24.9 ± 4.3	23.8 ± 2.6
Tb.Th (μm)	67.9 ± 3.2	60.2 ± 4.3	60.9 ± 5.9	61.7 ± 2.5
Tb.N (/mm)	3.7 ± 0.6	4.1 ± 0.3	4.1 ± 0.5	4.1 ± 0.4
Tb.Sp (mcm)	208.7 ± 43.3	182.7 ± 14.5	186.6 ± 31.9	194.5 ± 26.7
Ob.S/BS (%)	15.1 ± 1.3	13.4 ± 4.1	7.5 ± 0.8*#	4.1 ± 2.9*#
OS/BS (%)	22.0 ± 9.7	16.1 ± 4.0	7.7 ± 1.9*	4.3 ± 3.2*#
MS/BS (%)	31.9 ± 8.6	30.3 ± 9.1	30.0 ± 3.7	18.0 ± 4.4*
BFR/BS ($\mu\text{m}^3/\mu\text{m}^2/\text{y}$)	18.3 ± 5.2	10.2 ± 1.9*	7.0 ± 1.4*	5.2 ± 1.6*
Oc.S/BS (%)	20.4 ± 8.5	10.4 ± 3.4	9.5 ± 2.7*#	2.7 ± 1.1*#
ES/BS (%)	15.2 ± 5.5	8.5 ± 3.0	8.5 ± 2.9	6.9 ± 4.8*

BV/TV; bone volume per tissue volume, Tb.Th; trabecular thickness, Tb.N; trabecular number, Tb.Sp; trabecular separation, Ob.S/BS; osteoblast surface per bone surface, OS/BS; osteoid surface per bone surface, MS/BS; mineralized surface per bone surface, BFR/BS; bone formation rate per bone surface, Oc.S/BS; osteoclast surface per bone surface, ES/BS; eroded surface per bone surface.

* p < 0.05 versus TPTx rats.

p < 0.05 versus TPTx-1/2Nx rats.

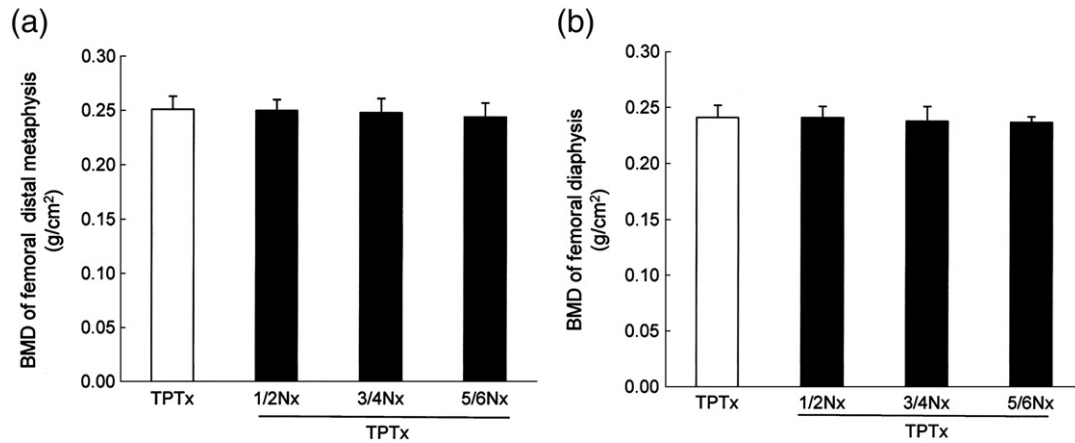


Fig. 6. Bone mineral density (BMD) in rat femur: (a) femoral distal metaphysis; (b) femoral diaphysis. There are no differences in BMD among all groups, both in distal metaphysis and diaphysis. TPTx; thyroparathyroidectomy, Nx; nephrectomy, TPTx-1/2Nx; thyroparathyroidectomized and 1/2 nephrectomized rats, TPTx-3/4Nx; thyroparathyroidectomized and 3/4 nephrectomized rats, TPTx-5/6Nx; thyroparathyroidectomized and 5/6 nephrectomized rats.

Bone mineral density assessed by DXA

In the right femur in which BMD was measured by DXA, BMD of the distal metaphysis and diaphysis regions were not different among four groups (Fig. 6).

Storage modulus assessed by DMA

Using DMA analysis, we evaluated the storage modulus in femoral diaphysis. Storage modulus at 1 Hz, was significantly decreased in TPTx-3/4Nx and TPTx-5/6Nx rats compared with TPTx rats. The storage modulus in the TPTx-5/6Nx group was reduced to 70% of the TPTx group. This decline in storage modulus appeared to depend slightly on the degree of renal dysfunction (Fig. 7a). The data of tan delta are shown in Fig. 7b.

Change in the chemical compositions of cortical bone

Analysis of the Raman spectra revealed that the resolvable mineral factor was carbonated apatite, almost identical to that reported by Tarnowski et al. [28]. Mineral properties such as carbonate to phosphate ratio and crystallinity were changed significantly in TPTx-5/6Nx rats (Figs. 8b and c). The cortical bone mineral to matrix ratio measured by v1 phosphate stretching vibration/amide I was significantly higher in TPTx-3/4Nx and TPTx-5/6Nx rats than in TPTx rats (Fig. 4a). Collagen

maturity (mature enzymatic crosslink to immature enzymatic crosslink) and pentosidine/amide increased significantly in TPTx-5/6Nx rats (Figs. 8d and e). Changes in all parameters were apparently dependent on the degree of renal dysfunction.

Contribution of changes in the chemical composition to mechanical property of cortical bone

Simple linear regression analyses were performed to elucidate the contribution of changes in chemical composition to alteration of mechanical property. Table 3 shows that all the chemical composition parameters tested (mineral/matrix, carbonate/phosphate, crystallinity, mature crosslinks/immature crosslinks, and pentosidine) were significantly associated with storage modulus, with carbonate to phosphate ratio having the weakest association. Using the above chemical composition parameters, we also performed stepwise multiple regression analysis. Table 4 shows that mature to immature crosslink ratio and crystallinity were independently associated with storage modulus.

Discussion

In this study, we demonstrated that CKD rat models with comparable PTH levels to control non-CKD rats have reduced storage modulus in cortical bone. Cortical bone is a viscoelastic material [29–31]. Past

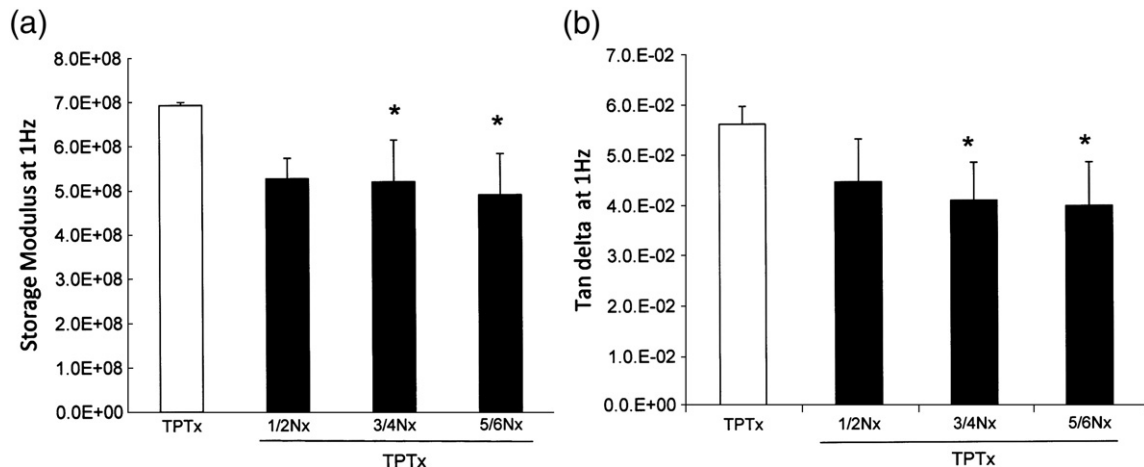


Fig. 7. Mechanical properties of rat femur assessed by dynamic mechanical analysis (DMA). (a) Storage modulus of rat femur at 1 Hz. Storage modulus decreases in TPTx-3/4Nx and TPTx-5/6 Nx groups compared to TPTx group. (b) Value of tan delta at 1 Hz. Significant decreases are observed in TPTx-3/4 and 5/6Nx groups compared to TPTx group. *p<0.05 versus TPTx rats.

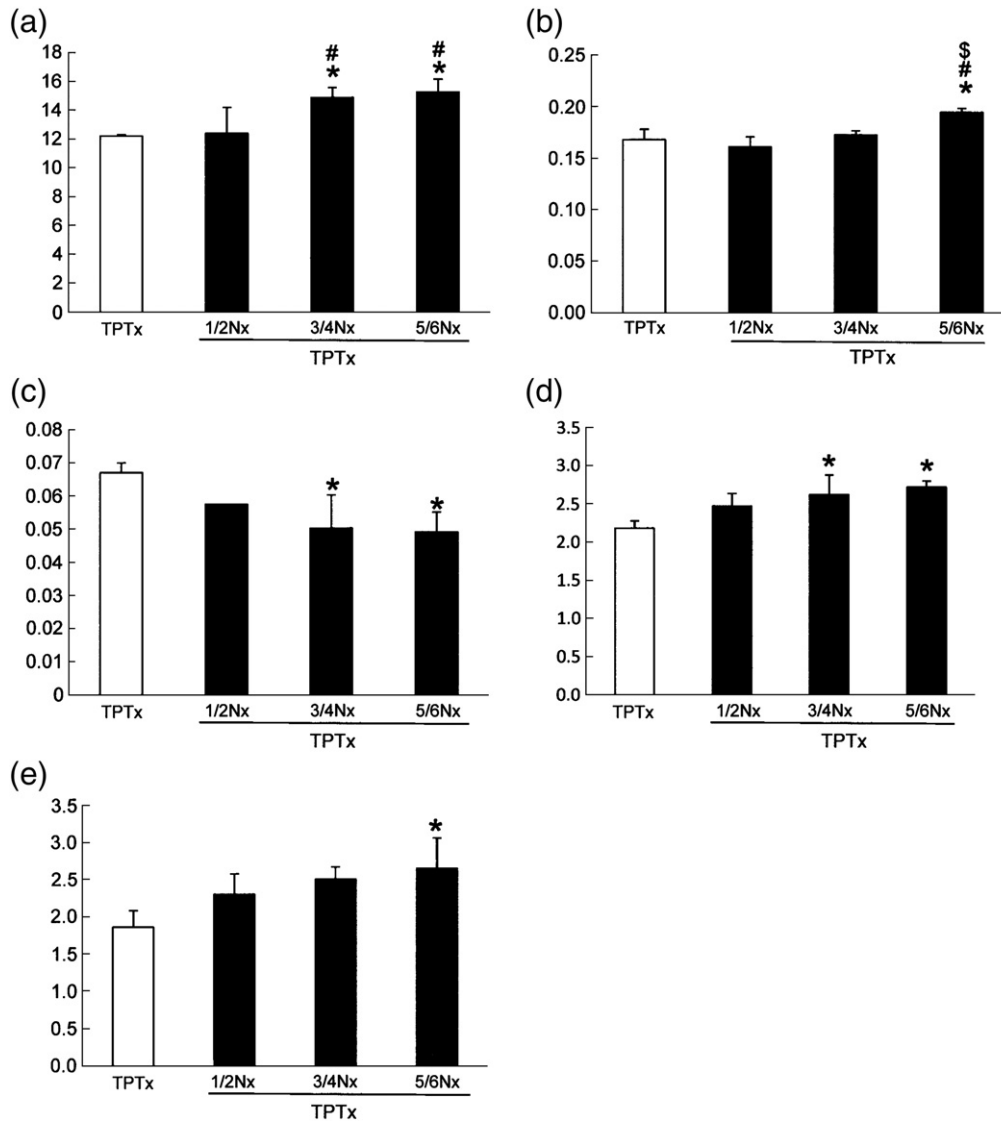


Fig. 8. Comparisons of bone material properties among the groups: (a) mineral to matrix ratio; (b) carbonate to phosphate ratio; (c) crystallinity; (d) mature crosslinks to immature crosslinks ratio; (e) pentosidine to matrix ratio. *p<0.05 versus TPTx rats. #p<0.05 versus TPTx-1/2Nx rats.

studies have shown that the viscoelastic properties of cortical bone correlate with the ultimate strength and toughness of tissue [29,32,33]. The strain rate dependence of compact bone can account for up to a fifth of the strength of the human femur during high speed loading [34]. Storage modulus obtained from DMA is equivalent to Young's modulus in a monotonical three-point bending test. Yamashita et al. [35] examined the conditions of DMA measurement in human cortical

bone samples, including level of stress, test duration, temperature, effect of sample size, and moisture. Their report demonstrated that DMA is a useful tool to test bone mechanical properties. Yeni et al. [36] also reported that DMA measurement can detect changes in mechanical property in bone specimens which have small yield damage. DMA is a nondestructive analysis and permits repeated analysis of the same sample. We therefore used this method to assess bone strength. Storage modulus in TPTx-Nx rats was reduced compared with TPTx rats. The two groups of animals had comparable Ca, PTH and BMD levels, and the difference in 1,25(OH)₂D₃ level was not significant. Although slightly altered vitamin D action may be another possible factor that changes

Table 3
Linear regression analyses of the relations between storage modulus and chemical composition.

Parameter	Regression equation	β	R ²	P value
Mineral/matrix	y = 1.1E + 009 - 4.2E + 007x	-0.654	0.428	0.001
Carbonate/phosphate	y = 1.1E + 009 - 3.1E + 009x	-0.450	0.202	0.027
Crystallinity	y = 1.2E + 008 + 7.9E + 009x	0.752	0.565	0.000
M. crosslinks/l. crosslinks	y = 1.4E + 009 - 3.2E + 008x	-0.794	0.631	0.000
Pentosidine	y = 8.2E + 008 - 3.0E + 008x	-0.681	0.464	0.000

y; storage modulus, x; chemical composition parameter.
Mineral/matrix; mineral to matrix ratio, carbonate/phosphate; carbonate to phosphate ratio, M. crosslinks/l. crosslinks; mature crosslinks to immature crosslinks ratio, β; coefficient of regression, R²; square of the correlation coefficient.

Table 4
Multiple regression analyses of the relations between storage modulus and chemical composition (N = 24).

Parameter	β	P value
M. crosslinks/l. crosslinks	-0.520	0.004
Crystallinity	0.387	0.028
Model R ²	0.709	0.000
Model adjusted R ²	0.681	0.000

M. crosslinks/l. crosslinks; mature crosslinks to immature crosslinks ratio, β; coefficient of regression, R²; square of the correlation coefficient.

bone material property under uremic condition, no significant differences in histomorphometric parameters of cancellous bone were observed between two groups, which strongly suggest no remarkable difference in cancellous bone connectivity [37]. A recent report demonstrated elevated fracture risk in early stage of CKD, which is independent of BMD [38]. Thus, the decreased bone strength found in TPTx–Nx rats is likely to be derived from changes in bone quality and not reduction in bone mass in this model. Since the results suggested no obvious difference in the structural property, we speculated that the most significant causative factor may be changes in material property, especially the chemical composition of bone matrix, in this disease model.

Therefore we used vibrational spectroscopy to analyze the chemical composition of cortical bone in femoral diaphysis, at the same region where storage modulus was measured. We found increases in mineral to matrix ratio and carbonate substitution in TPTx–Nx rats. Increases in these two parameters have been observed in low bone turnover induced by aging [39] and bisphosphonate therapy [40]. We previously reported that TPTx–Nx rats demonstrate lower bone turnover than TPTx rats [20]. In this study, histomorphometric analysis revealed that TPTx–Nx rats have lower bone turnover. The above-mentioned changes may be associated with lowered bone turnover. Recently, Boskey et al. [41] reported that increased cortical mineral to matrix ratio was associated with increased fracture risk. Too high a mineral content is known to render bones more brittle. Furthermore, increased carbonate to phosphate ratio is associated with decreased elastic modulus in rat femur [42]. Goldstein et al. [18] observed increased carbonate to phosphate ratio in cortical bone in older people aged above 50 with fracture. These results support our notion that reduced storage modulus in TPTx–Nx rats may be caused by elevated mineral to matrix ratio and carbonate to phosphate ratio in this study.

In addition, we observed reduced crystallinity in TPTx–Nx rats in this study. Akkus et al. [18,24,42] demonstrated reduced crystallinity and increased carbonate to phosphate ratio in low turnover bones in aged rats. They also reported an inverse relationship between crystallinity and degree of carbonation substitution [43] as well as an association between crystallinity and elastic modulus [18,43]. Therefore, it is possible that the reduced storage modulus in our model rats may be caused by the changes in mineral properties.

On the other hand, parameter of collagen maturity, which is calculated as the ratio of mature enzymatic crosslink to immature enzymatic crosslink, and non-enzymatic crosslink pentosidine increased in TPTx–5/6Nx rats in this study. Previous studies revealed that increasing crosslink ratio was associated with bone fragility [41,44]. Moreover previous studies reported an association between bone fragility and the amount of pentosidine in bone [45–48], serum [49] and urine [50,51]. Saito et al. [45–48] revealed that accumulation of pentosidine in bone was associated with bone fracture. Other groups also reported that pentosidine in bone was associated with mechanical properties such as ultimate strain [52], failure load, and work to fracture [53]. In our study, we observed a significant increase in pentosidine to matrix ratio in TPTx–Nx rats, and the amount showed an apparent inverse relationship with both renal function and bone turnover (Fig. 6). Advanced glycation end product cross-links including pentosidine are markedly increased via oxidative reactions [54] even when bone turnover rates and glycemic control are within normal ranges [55]. We did not measure markers of glucose metabolism in our study. However, the main cause of pentosidine accumulation in our chronic kidney injury model would be uremia rather than abnormal glucose metabolism, because pentosidine is also markedly elevated in plasma protein and skin collagen fiber of uremic patients, regardless of glycemic control or tissue turnover rate. In uremia, accumulation of pentosidine is a result of increased oxidative stress [56]. Therefore, increased pentosidine to matrix ratio in the cortical bone of TPTx–Nx rats may reflect increased oxidative stress associated with renal dysfunction. Thus, uremia-related oxidative stress may alter bone mechanical properties by increasing

pentosidine in bone matrix. Additionally, lowered bone turnover may contribute to the increased pentosidine to matrix ratio because of we observed an increase of this parameter in TPTx–5/6Nx rats that had lowered bone turnover.

To determine whether changes in chemical composition contribute to alteration of storage modulus, we performed simple linear regression and multiple regression analyses. As shown in Table 4, multiple regression analyses identified two chemical composition parameters; mature to immature crosslink ratio and crystallinity, as independently contributing to bone strength, whereas mineral/matrix ratio and pentosidine were not independent contributors in this model. However, the validity of these results may be limited because they were obtained from a relatively small number of animals with early kidney dysfunction. Further studies are required to confirm the independent contribution of each chemical composition parameter to change in mechanical property.

In conclusion, the mechanical property of femoral cortical bone was deteriorated in rats with impaired kidney function but no excessive PTH secretion. In these rats, BMD and cancellous bone microstructure were unchanged, but chemical compositions of bone matrix including mineral and collagen enzymatic and non-enzymatic crosslinks were altered accompanying degeneration of renal function. Therefore chemical composition alterations in cortical bone are likely to be the major pathogenesis of bone fragility in CKD. Uremia-related oxidative stress or yet unknown uremic toxins may exacerbate these chemical changes, which would further deteriorate bone mechanical properties in renal dysfunction states.

Conflict of interest declaration

There is no conflict of interest in connection with the present study and submission.

Acknowledgments

Standard sample of pentosidine was provided by Dr. Ryoji Nagai (Japan Women's University, Japan). We are grateful to Dr. Minako Wakasugi (Niigata University) and Dr. Keiichiro Saiki (Oita University of Nursing and Health Sciences) for statistical analyses, and also to Dr. Kiyoshi Miyashita (Gunma Industrial Technology Center) for technical advice on Raman spectroscopy measurement. This work was supported in part by grants from the Kidney Foundation Japan (to Iwasaki Y). Part of this work was presented and received the Young Investigator Award of the Japanese Society of Bone Morphometry (2010).

References

- [1] Alem AM, Sherrard DJ, Gillen DL, Weiss NS, Beresfold SA, Heckbert SR, et al. Increased risk of hip fracture among patients with end-stage renal disease. *Kidney Int* 2000;58:396–9.
- [2] CoCo M, Rush H. Increased incidence of hip fracture s in dialysis patients with low serum parathyroid hormone. *Am J Kidney Dis* 2000;36:1115–21.
- [3] Nickolas TL, McMahon DJ, Shane E. Relationship between moderate to severe kidney disease and hip fracture in the United States. *J Am Soc Nephrol* 2006;17:3223–32.
- [4] Ensrud KE, Lui LY, Taylor BC, Ishani A, Shlipak MG, Stone KL, et al. Osteoporotic Fracture Research Group. Renal function and risk of hip and vertebral fractures in older women. *Arch Intern Med* 2007;167:133–9.
- [5] Jamal SA, Bauer DC, Ensrud KE, Cauley JA, Hochberg M, Ishani A, et al. Alendronate treatment in women with normal to severe renal impaired renal function: an analysis of the fracture intervention trial. *J Bone Miner Res* 2007;22:503–8.
- [6] Fried LF, Biggs ML, Shlipak MG, Seliger S, Kestenbaum B, Stehman-Breen C, et al. Association of kidney function with incident hip fracture in older adults. *J Am Soc Nephrol* 2007;18:282–6.
- [7] Dooley AC, Weiss NS, Kestenbaum B. Increased risk of hip fracture among men with CKD. *Am J Kidney Dis* 2008;51:38–44.
- [8] Mittalhenkle A, Gillen DL, Stehman-Breen CO. Increased risk of mortality associated with hip fracture in the dialysis population. *Am J Kidney Dis* 2004;44:672–9.

- [9] Nitsch D, Mylne A, Roderick PJ, Smeeth L, Hubbard R, Fletcher A. Chronic kidney disease and hip fracture-related mortality in older people in the UK. *Nephrol Dial Transplant* 2009;24:1539–44.
- [10] Jassal SK, Muhlen D, Barrett-Connor E. Measures of renal function, BMD, bone loss, and osteoporotic fracture in older adults: the Rancho Bernardo Study. *J Bone Miner Res* 2007;22:203–10.
- [11] Fusaro M, D'Angel A, Scalzo G, Gallieni M, Giannini S, Guglielmi G. Vertebral fractures in dialysis: endocrinological disruption of the bone–kidney axis. *J Endocrinol Invest* 2010;33:347–52.
- [12] Parfitt AM. A structural approach to renal bone disease. *J Bone Miner Res* 1998;13:1213–20.
- [13] Rudse KD, de Boer IH, Dooley A, Young B, Kestenbaum B. Fracture risk after parathyroidectomy among chronic hemodialysis patients. *J Am Soc Nephrol* 2007;18:2401–7.
- [14] Nakai S, Masakane I, Shigematsu T, Hamano T, Yamagata K, Watanabe Y, Itami N, Ogata S, Kimata N, Shinoda T, Shoji T, Suzuki K, Taniguchi M, Tsuchida K, Nakamoto H, Nishi S, Nishi H, Hashimoto S, Hasegawa T, Hanafusa N, Fujii N, Marubayashi S, Morita O, Wakai K, Wada A, Iseki K, Tsubakihara Y. An overview of regular dialysis treatment in Japan (as of 31 December 2008). *Ther Apher Dial* 2010;14:505–40.
- [15] Seeman E, Delmas PD. Bone quality—the material and structural basis of bone strength and fragility. *N Engl J Med* 2006;354:2250–61.
- [16] Fratzl P, Gupta HS, Paschalis EP, Roschger P. Structure and mechanical quality of the collagen–mineral nano-composite in bone. *J Mater Chem* 2004;14:2115–23.
- [17] Weiner S, Wagner HD. The material bone: structure–mechanical function relations. *Annu Rev Mater Sci* 1998;28:271–98.
- [18] Yerramshetty JS, Akkus O. The associations between mineral crystallinity and the mechanical properties of human cortical bone. *Bone* 2008;42:476–82.
- [19] McCreddie BR, Morris MD, Chen TC, Sudhaker Rao D, Finney WF, Widjaja E, et al. Bone tissue compositional differences in women with and without osteoporotic fracture. *Bone* 2006;39:1190–5.
- [20] Iwasaki-Ishizuka Y, Yamato H, Nii-kono T, Kurokawa K, Fukagawa M. Down-regulation of parathyroid hormone receptor gene expression and osteoblastic dysfunction associated with skeletal resistance to parathyroid hormone in a rat model of renal failure with low turnover bone. *Nephrol Dial Transplant* 2005;20:1904–11.
- [21] Parfitt AM, Drezner MK, Glorieux FH, Kanis JA, Malluche H, Meunier PJ, et al. Bone histomorphometry: standardization of nomenclature, symbols, and units. Report of the ASBMR Histomorphometry Nomenclature Committee. *J Bone Miner Res* 1987;2:595–610.
- [22] Menard KP. Dynamic mechanical analysis: a practical introduction. New York: CRC Press; 2008. p. 1–15.
- [23] Faibish D, Ott SM, Boskey AL. Mineral changes in osteoporosis: a review. *Clin Orthop Relat Res* 2006;443:28–38.
- [24] Yerramshetty JS, Lind C, Akkus O. The compositional and physicochemical homogeneity of male femoral cortex increases after the sixth decade. *Bone* 2006;29:1236–43.
- [25] Carden A, Rajachar RM, Morris MD, Kohn DH. Ultrastructural changes accompanying the mechanical deformation of bone tissue: a Raman imaging study. *Calcif Tissue Int* 2003;72:166–75.
- [26] Miyazaki K, Nagai R, Horiuchi S. Creatine plays a direct role as a protein modifier in the formation of a novel advanced glycation end product. *J Biochem* 2002;132:543–50.
- [27] Glenn JV, Beattie JR, Barrett L, Frizzell N, Thorpe SR, Boulton ME, et al. Confocal Raman microscopy can quantify advanced glycation end product (AGE) modifications in Bruch's membrane leading to accurate, nondestructive prediction of ocular aging. *FASEB J* 2007;21:3542–52.
- [28] Tarnowski CP, Ignelzi MA, Morris MD. Mineralization of developing mouse calvaria as revealed by Raman microspectroscopy. *J Bone Miner Res* 2002;17:1118–26.
- [29] Carter DR, Hays WC. The compressive behavior of bone as a two-phase porous structure. *J Bone Joint Surg Am* 1997;59:954–62.
- [30] Garner E, Lakes R, Lee T, Swan C, Brand R. Viscoelastic dissipation in compact bone: implications for stress-induced fluid flow in bone. *J Biomech Eng* 2000;122:166–72.
- [31] McElhaney JH. Dynamic response to bone and muscle tissue. *J Appl Physiol* 1966;21:1231–6.
- [32] Currey JD. Strain rate and mineral content in fracture models of bone. *J Orthop Res* 1988;6:32–8.
- [33] Robertson DM, Smith DC. Compressive strength of mandibular bone as a function of microstructure and strain rate. *J Biomech* 1987;11:455–7.
- [34] Coutney AC, Wachtel EF, Myers ER, Hayes WC. Effect of loading rate on strength of the proximal femur. *Calcif Tissue Int* 1994;55:53–8.
- [35] Yamashita J, Furman BR, Rawls HR, Wang X, Agrawal CM. The use of dynamic mechanical analysis to assess the viscoelastic properties of human cortical bone. *J Biomed Mater Res* 2001;59:47–53.
- [36] Yeni YN, Shaffer R, Baker KC, Dong XN, Grimm MJ, Les CM, et al. The effect of yield damage on the viscoelastic properties of cortical bone tissue as measured by dynamic mechanical analysis. *J Biomed Mater Res* 2007;82:530–7.
- [37] Kazama JJ, Koda R, Yamamoto S, Narita I, Gejyo F, Tokumoto A. Cancellous bone volume is an indicator for trabecular bone connectivity in dialysis patients. *Clin J Am Soc Nephrol* 2010;5:292–8.
- [38] Kaji H, Yamauchi M, Yamaguchi T, Shigematsu T, Sugimoto T. Mild renal dysfunction is a risk factor for a decrease in bone mineral density and vertebral fractures in Japanese postmenopausal women. *J Clin Endocrinol Metab* 2010;95:4635–42.
- [39] Gourion-Arsiquaud S, Burket JC, Havill LM, DiCarlo E, Doty SB, Mendelsohn R, et al. Spatial variation in osteonal bone properties relative to tissue and animal age. *J Bone Miner Res* 2009;24:1271–81.
- [40] Boskey AL, Spevak L, Weinstein RS. Spectroscopic markers of bone quality in alendronate-treated postmenopausal women. *Osteoporos Int* 2009;20:793–800.
- [41] Gourion-Arsiquaud S, Faibish D, Myers E, Spevak L, Compston J, Hodsman A, et al. Use of FTIR spectroscopic imaging to identify parameters associated with fragility fracture. *J Bone Miner Res* 2009;24:1565–71.
- [42] Akkus O, Adar F, Shaffler MB. Age-related changes in physicochemical properties of mineral crystals are related to impaired mechanical function of cortical bone. *Bone* 2004;34:443–53.
- [43] Akkus O, Akkus-Polyakova A, Adar F, Schaffler M. Aging of microstructural compartments in human compact bone. *J Bone Miner Res* 2003;18:1012–9.
- [44] Paschalis EP, Shane E, Lyritis G, Skarantavos G, Mendelsohn R, Boskey AL. Bone fragility and collagen cross-links. *J Bone Miner Res* 2004;19:2000–4.
- [45] Saito M, Fujii K, Soshi S, Tanaka T. Reductions in degree of mineralization and enzymatic collagen cross-links and increases in glycation-induced pentosidine in the femoral neck cortex in cases of femoral neck fracture. *Osteoporos Int* 2006;17:986–95.
- [46] Saito M, Fujii K, Mori Y, Karumo K. Role of collagen enzymatic and glycation induced cross-links as a determinant of bone quality in spontaneously diabetic WBN/Kob rats. *Osteoporos Int* 2006;17:1514–23.
- [47] Saito M, Fujii K, Marumo K. Degree of mineralization-related collagen crosslinking in the femoral neck cancellous bone in cases of hip fracture and controls. *Calcif Tissue Int* 2006;79:160–8.
- [48] Saito M, Marumo K. Collagen cross-links as a determinant of bone quality: a possible explanation for bone fragility in aging, osteoporosis, and diabetes mellitus. *Osteoporos Int* 2010;21:195–214.
- [49] Yamamoto M, Yamaguchi T, Yano S, Sugimoto T. Serum pentosidine are positively associated with the presence of vertebral fractures in postmenopausal women with type 2 diabetes. *J Clin Endocrinol Metab* 2008;93:10013–1919.
- [50] Shiraki M, Kuroda T, Tanaka S, Saito M, Fukunaga M, Nakamura T. Nonenzymatic collagen cross-links induced by glycoxidation (pentosidine) predicts vertebral fractures. *J Bone Miner Res* 2008;26:93–100.
- [51] Schwartz AV, Garner P, Hillier TA, Sellmeyer DE, Strotmeyer ES, Feingold KR, et al. Pentosidine and increased fracture risk in older adults with type 2 diabetes. *J Clin Endocrinol Metab* 2009;94:2380–6.
- [52] Hernandez C, Tang SY, Baumbach BM, Hwu PB, Sakkee AN, van der Ham F, et al. Trabecular microfracture and influence of pyridinium and non-enzymatic glycation-mediated collagen cross-links. *Bone* 2005;37:825–32.
- [53] Viguet-Carrin S, Roux JP, Arlot ME, Merabet Z, Leeming DJ, Byrjalsen I, et al. Contribution of the advanced glycation end product pentosidine and of maturation of type I collagen to compressive biomechanical properties of human lumbar vertebrae. *Bone* 2006;39:1073–9.
- [54] McCarthy AD, Etcheverry SB, Bruzzone L, Lettieri G, Barrio DA, Cortizo AM. Non-enzymatic glycation of type I collagen matrix: effect on osteoblastic development and oxidative stress. *BMC Cell Biol* 2001;2:16.
- [55] Saito M, Marumo K, Soshi S, Kida Y, Ushiku C, Shinohara A. Raloxifene ameliorates detrimental enzymatic and nonenzymatic collagen cross-links and bone strength in rabbits with hyperhomocysteinemia. *Osteoporos Int* 2010;21:655–66.
- [56] Miyata T, van Ypersele de Strihou C, Kurokawa K, Baynes JW. Alternations in nonenzymatic biochemistry in uremia: origin and significance of "carbonyl stress" in long-term uremic complications. *Kidney Int* 1999;55:389–99.